

## Strong $\mathbf{E} \times \mathbf{B}$ Flow Shear and Reduced Fluctuations in a Reversed-Field Pinch

B. E. Chapman, C.-S. Chiang, S. C. Prager, J. S. Sarff, and M. R. Stoneking

*Department of Physics, University of Wisconsin, Madison, Wisconsin 53706*

(Received 8 May 1997)

Large radial electric field gradients, leading to sheared  $\mathbf{E} \times \mathbf{B}$  flow, are observed in enhanced confinement discharges in the Madison Symmetric Torus reversed-field pinch. The flow shear develops in a narrow region in the plasma edge. Electrostatic fluctuations are reduced over the entire plasma edge with an extra reduction in the shear region. Magnetic fluctuations, resonant in the plasma core but global in extent, are also reduced. The reduction of fluctuations in the shear region is presumably due to the strong shear, but the causes of the reductions outside this region have not been established. [S0031-9007(98)05480-5]

PACS numbers: 52.55.Hc, 52.25.Fi, 52.25.Gj, 52.35.Qz

The reversed-field pinch (RFP) is a magnetically confined toroidal plasma configuration characterized by a relatively weak toroidal magnetic field whose direction in the plasma edge is opposite that in the core. There is also a poloidal magnetic field whose strength is comparable to that of the toroidal field. Fluctuations in the magnetic field have been measured to drive particle [1] and energy [2] transport in the plasma core, and reduction of magnetic fluctuations has been linked to recent improvements in particle and energy confinement [3,4]. Fluctuations in the electric field have been measured to drive particle transport in the plasma edge [5], but the mechanism underlying energy transport in the edge has not been established. In general, magnetic fluctuations are believed to play a larger role than electrostatic fluctuations in determining RFP global transport.

In contrast to the RFP is the tokamak configuration, which has a strong, stabilizing toroidal magnetic field and weak magnetic fluctuations. Electrostatic fluctuations are believed to drive the bulk of particle and energy transport in the tokamak. In this magnetic configuration (and others) electrostatic fluctuations and transport have been reduced by the generation of strongly sheared  $\mathbf{E} \times \mathbf{B}$  plasma flow attributed to inhomogeneity in the radial electric field [6,7].

In this Letter, we report observations of a strongly inhomogeneous radial electric field, leading to sheared  $\mathbf{E} \times \mathbf{B}$  flow, in the RFP. The shear develops in a narrow region in the edge of enhanced confinement discharges in which the energy confinement time can reach triple the normal value [8]. Also observed in these discharges is a broadband reduction of electrostatic fluctuations over the entire plasma edge with an extra reduction in the shear region. Magnetic fluctuations, resonant in the core but global in extent, are also reduced. The reduction of electrostatic fluctuations in the shear region is presumably due to the strong shear, but the causes of the reductions outside this region have not been determined. Also yet to be determined is the relative contribution to enhanced confinement from each fluctuation reduction.

These observations were made in the Madison Symmetric Torus (MST) [9] RFP. The Ohmically heated MST

plasma has a major radius of 150 cm and a minor radius of 51 cm, determined by graphite limiters mounted on the plasma-facing wall. Periods of enhanced confinement occur subject to constraints on toroidal field reversal, electron density, wall conditioning, and fueling.

The most important requirements for enhanced confinement discharges are sufficiently low density and sufficiently strong toroidal field reversal, the latter represented by  $F \equiv B_\phi(a)/\langle B_\phi \rangle$ , where  $B_\phi(a)$  is the toroidal field at the edge, and  $\langle B_\phi \rangle$  is the cross-section average. The reversal and density requirements relax with increasing plasma current,  $I_\phi$ . For example, at  $I_\phi \sim 200$  kA, the minimum (least negative)  $F \sim -0.5$ , and the maximum line-averaged density,  $\langle n_e \rangle \sim 6 \times 10^{12} \text{ cm}^{-3}$ . At 500 kA, the minimum  $F \sim -0.2$ , and the maximum  $\langle n_e \rangle \sim 1.2 \times 10^{13} \text{ cm}^{-3}$ . Enhanced confinement discharges requiring strong toroidal field reversal were also observed in the TPE-1RM20 RFP [10]. Magnetic fluctuations were reduced in these discharges, but neither electrostatic fluctuations nor the radial electric field profile were measured.

Enhanced confinement discharges in the MST also require conditioning of the plasma-facing wall, by boronization and/or pulsed discharge cleaning [8,11]. The fueling technique also plays a role, as wall fueling (e.g., recycling) is preferred over gas puff fueling.

Enhanced confinement was initially attributed to a suppression of confinement-degrading sawtooth crashes [8]. However, we subsequently observed crash suppression in weakly reversed discharges *without* enhanced confinement. We also found that, unlike strongly reversed discharges, weakly reversed discharges lack strong  $\mathbf{E} \times \mathbf{B}$  flow shear and reduced fluctuations.

The differences between standard (low) and enhanced confinement are illustrated with a single discharge in Fig. 1, which contains the central electron temperature, indicated roughly by soft x-ray emission, the Ohmic input power ( $P_{\text{Oh}}$ ), and the emission from one edge impurity species. A brief period of enhanced confinement ending at about 9 ms is followed by a longer one starting at about 11 ms. A period of standard confinement begins with the sawtooth crash [8,12] after 16 ms. With enhanced

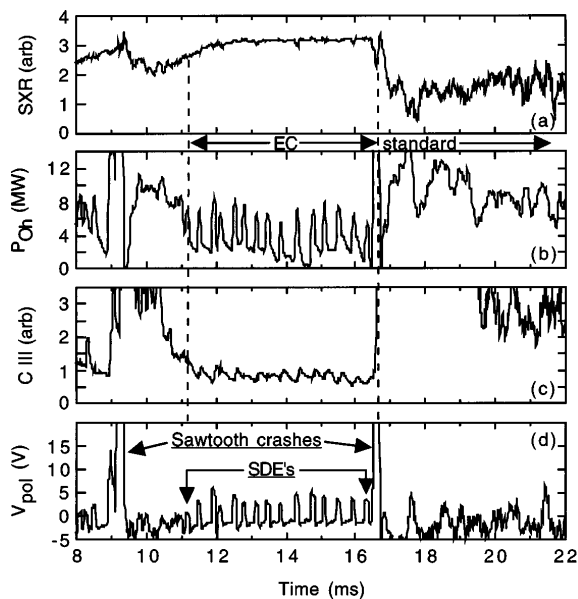


FIG. 1. (a) The ratio of two soft x-ray signals  $\propto$  core electron temperature, (b) Ohmic input power, (c) C III (464.7 nm) radiation, and (d) surface poloidal voltage in a discharge with a period of enhanced confinement (EC) followed by a period of standard confinement. Small dynamo events (SDE's) occur throughout the EC period. There is also a brief EC period ending at 9 ms.

confinement, the central electron temperature is higher,  $P_{Oh}$  is lower, and radiation power loss from edge impurities and neutral fuel atoms ( $H_\alpha$ , not shown) is reduced.

Because of the increase in stored thermal energy and the reduction of  $P_{Oh}$ , the enhanced energy confinement time,  $\tau_E \equiv$  (stored thermal energy)/(Ohmic input power) is  $\geq 3$  ms, a roughly threefold improvement over the standard  $\tau_E$  of 1 ms [8]. Note that the enhanced  $\tau_E$  averages over small dynamo events (described in the next paragraph), which momentarily degrade confinement. Accompanying the improved energy confinement is a poloidal beta  $\equiv$  (plasma thermal pressure)/(edge poloidal magnetic pressure) of  $\geq 7\%$ . The particle confinement time is unknown due to uncertainty in the particle source rate, but low  $H_\alpha$  (or  $D_\alpha$ ) radiation and a constant or rising  $\langle n_e \rangle$  indicate that particle confinement likely improves.

Sawtooth crashes are observed in the surface poloidal voltage [Fig. 1(d)], which increases with an increase in the toroidal flux in the plasma volume. Thus, sawtooth crashes are dynamo events, characterized by the generation of poloidal plasma current and toroidal flux. During periods of enhanced confinement, dynamo events occur with substantially lower amplitude than sawtooth crashes, and unlike sawtooth crashes, which originate in core-resonant  $m = 1$  magnetic fluctuations, these small dynamo events originate in edge-resonant  $m = 0$  magnetic fluctuations [8].

Most of the data discussed in the remainder of this Letter was gathered using probes inserted into the edge of MST plasmas with  $I_\phi = 200$  kA and  $\langle n_e \rangle \sim 5 \times 10^{12}$  cm $^{-3}$ . Magnetic sensing probes were used to measure  $\mathbf{B}(r)$ , and

Langmuir probes were used to measure radial profiles of  $V_p$  (plasma potential),  $E_r$  (radial electric field)  $= -\nabla(V_p)$ ,  $V_f$  (floating potential), and  $J_s$  (ion saturation current).  $V_p$  was measured using the swept probe technique. On each of the Langmuir probes a shield was installed to block the small population of superthermal (fast) electrons present in the plasma edge [1]. Fast electrons can render the probe signals unreliable (e.g., from the sudden onset of thermionic electron emission) and lead to rapid destruction of the probes. Comparisons of Langmuir probe data with and without the shield show that its presence does not significantly affect the shape of the equilibrium profiles. Each data point in the profiles presented below is an ensemble average of time-averaged data from 10–30 similar discharges. The time windows are of varying length, chosen to avoid sawtooth crashes but averaging over small dynamo events in the enhanced confinement case. Error bars represent the statistical variation in the ensemble averages.

The radial electric field and its gradients are relatively small in standard (low confinement) discharges, but both become large in a narrow region in the edge of enhanced confinement discharges. The profiles of  $V_p(r)$  and  $E_r(r)$  for both cases are shown in Fig. 2. The shear in  $\mathbf{B}$  is relatively weak in the plasma edge, so  $E_r(r)$  approximates the shape of the  $\mathbf{E} \times \mathbf{B}$  flow profile. The maximum in  $E_r$  lies about 5 cm outside of the toroidal field reversal radius (across which the toroidal field changes direction). The positive  $E_r$  (pointing out of the plasma) in the shear region is in contrast to the negative  $E_r$  typical of the shear region in tokamaks and other devices [6], except in the case where a positive  $E_r$  was imposed with an insertable biased probe [13].

From the radial force balance equation,  $E_r = \nabla P(nZe)^{-1} - (\mathbf{V} \times \mathbf{B})_r$ , the radial electric field is a function of the local pressure gradient ( $\nabla P$ ) and fluid velocity ( $\mathbf{V}$ ) [14]. For majority ions, the typical pressure gradient makes a negative contribution to  $E_r$ , thus implying for the MST that the (as yet unmeasured)  $\mathbf{V} \times \mathbf{B}$  term must make a large positive contribution. As there is no external source of momentum input,  $\mathbf{V}$  must be self-generated.

The floating and plasma potentials (Fig. 2) are related by  $V_f = V_p - \alpha T_e$ , where  $\alpha$  is  $\sim$  constant, and  $T_e$  is the electron temperature. Thus, for a reasonable  $T_e(r)$ , increasing with decreasing minor radius, the positive jump in  $V_f$  is consistent with the jump in  $V_p$ . In standard discharges [Fig. 2(g)], there is no increase in  $V_p$ , and  $V_f$  decreases steadily with decreasing radius. With  $\alpha = 2.5$  (calculated from MST parameters), one estimates  $T_e(46 \text{ cm}) \sim 16$  eV and  $T_e(44 \text{ cm}) \sim 32$  eV for the enhanced confinement case, suggesting that the electron temperature doubles going from outside to inside the region of strong shear. However, these numbers very likely underestimate  $T_e$ , as effects such as secondary electron emission add a positive offset to  $V_f$  everywhere.

Comparing the enhanced confinement and standard profiles in Figs. 2(d) and 2(h),  $J_s \sim n_e T_e^{1/2}$  and  $\nabla J_s$  are both

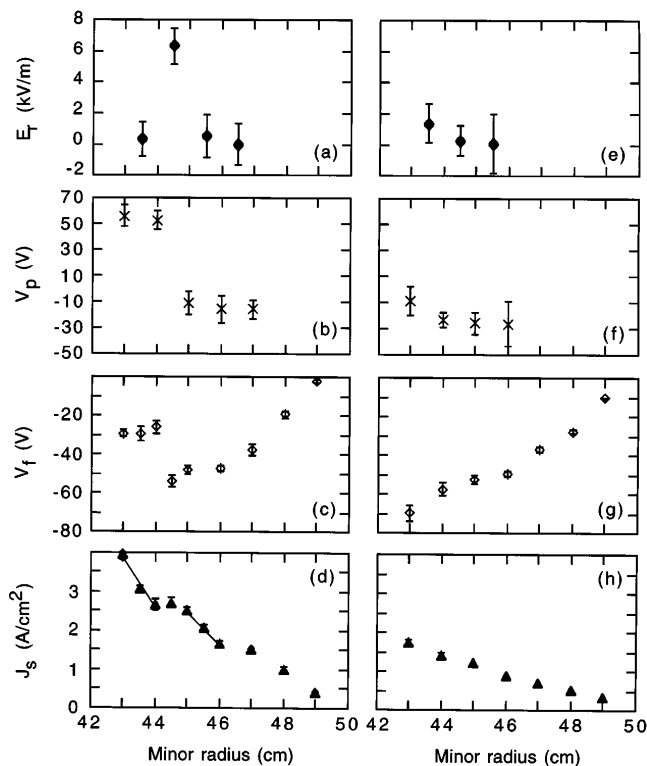


FIG. 2. Profiles of (a) radial electric field, (b) plasma potential, (c) floating potential, and (d) ion saturation current in enhanced confinement discharges. Profiles in (e)–(h) are for standard (weakly reversed) discharges. The plasma edge is at 51 cm.

larger in the enhanced confinement case over most of the plasma edge, implying that  $\nabla n_e$  and/or  $\nabla T_e$  are larger. The enhanced confinement profile is steepest in two locations (indicated by solid lines) that overlap the shear region, but it is flat in the center of the shear region. The increase of  $\nabla n_e$  and/or  $\nabla T_e$  in the region of strong shear is consistent with this region acting as a barrier to transport [the local flattening of  $J_s(r)$  where  $E_r$  peaks may result from a minimum in the flow shear].

The reduction of electrostatic and magnetic fluctuations during a period of enhanced confinement is shown in Fig. 3. The floating potential measured 2 cm from the plasma edge is shown in Fig. 3(a), and in Fig. 3(b) is shown the normalized rms fluctuation in the magnetic field,  $b_{rms}$ , measured with an array of magnetic pickup coils at the plasma edge. Before and after the period of enhanced confinement, fluctuation levels are substantial, and confinement is degraded. The surface poloidal voltage is included in Fig. 3(c) to show the timing of the small dynamo events. Each event momentarily increases fluctuations, but the time between events, which can be as short as  $\sim 0.1$  ms (e.g., refer to Fig. 1 around 12 ms), is relatively long in this discharge, and the time-averaged fluctuation amplitudes are particularly low.

The dominant contributors to  $b_{rms}$  are core-resonant global tearing modes with poloidal mode number  $m = 1$  and toroidal mode numbers  $n = 6-10$ . Also important

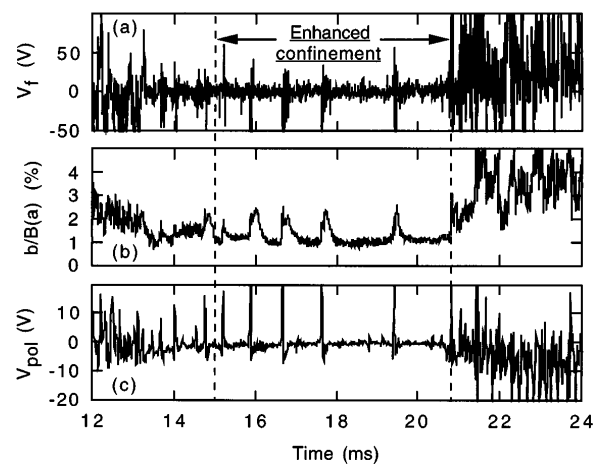


FIG. 3. (a) The floating potential 2 cm from the plasma edge, (b) rms fluctuation in the magnetic field normalized to the total field at the edge, and (c) surface poloidal voltage during a discharge with a period of enhanced confinement.

is the  $(m, n) = (0, 1)$  mode, resonant at the toroidal field reversal radius near the plasma edge. The  $(0, 1)$  amplitude, and  $b_{rms}$ , increase momentarily with each small dynamo event [8]. A common feature of the  $m = 1$  modes during enhanced confinement is that their normally steady growth between sawtooth crashes is absent [8]. In some discharges, like the one in Fig. 3,  $b_{rms}$  drops to  $\sim 1\%$  between small dynamo events. This is close to the record low  $b_{rms} \sim 0.8\%$  achieved recently in the MST when edge auxiliary poloidal current was applied with the goal of reducing  $b_{rms}$  [4].

The reduction of electrostatic fluctuations during enhanced confinement occurs over the entire edge plasma and over a broad range of frequencies (1–250 kHz). This is illustrated in Fig. 4. The enhanced confinement and standard profiles of the total fluctuation power in  $V_f$  are shown in Fig. 4(a). These profiles result from frequency integration over the ensemble power spectrum at each radius. Also shown is the enhanced confinement profile of  $E_r$  from Fig. 2(a). In addition to the roughly tenfold reduction of fluctuation power over the entire edge plasma, the enhanced confinement profile also exhibits a further reduction in the region of strong shear. The two local reductions in the standard profile may arise from the fact that only global data such as  $P_{Oh}$  are used for classification of standard and enhanced confinement discharges [we are unable to measure  $E_r(r)$  in a single discharge]. One can identify enhanced confinement without ambiguity, but some standard discharges may possess local fluctuation reduction without a reduction of  $P_{Oh}$ , producing the ensemble profile in Fig. 4(a).

The reduction of electrostatic fluctuations in the shear region can occur due to the strong shear if the  $\mathbf{E} \times \mathbf{B}$  flow shearing rate is larger than the rate of turbulent radial scattering of fluctuations due to the ambient turbulence (in the absence of  $\mathbf{E} \times \mathbf{B}$  flow shear) [15–17]. This is referred to as the strong shear criterion. For enhanced

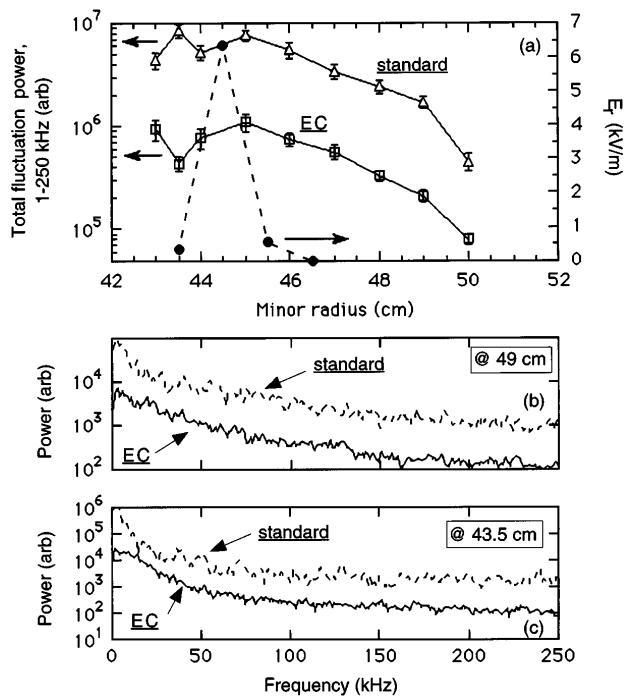


FIG. 4. (a) Profiles of enhanced confinement (EC) radial electric field and total fluctuation power in the floating potential, (b) EC and standard power spectra at 49 cm, and (c) EC and standard power spectra at 43.5 cm. Spectra are frequency integrated to derive the total fluctuation power in (a). "Standard" refers to low confinement periods of strongly reversed discharges. The plasma edge is at 51 cm.

confinement discharges in the MST, the shearing rate  $\omega_s \approx (1/B)\partial E_r/\partial r \sim 7 \times 10^6 \text{ s}^{-1}$ . The ambient turbulence scattering rate, estimated from the width of the standard power spectrum in Fig. 4(c), is  $\sim 3 \times 10^5 \text{ s}^{-1}$ . Thus, enhanced confinement discharges are in the strong shear regime. Further, the local magnetic field shear is sufficient to prevent Kelvin-Helmholtz instability, which can arise in the presence of any sheared mass flow [15,17]. We are as yet unable to measure the time dependence of  $E_r(r)$ , but measurements of the time evolution of the floating potential profile (related to the radial electric field profile) with a multitipped probe indicate that the strong  $\mathbf{E} \times \mathbf{B}$  flow shear develops  $\geq 1$  ms before the fluctuations are reduced. In Fig. 3(a), for example, the strong shear would emerge just after 12 ms.

The strong shear criterion applies strictly to high frequency (short wavelength) fluctuations lying entirely within the shear region [15], but the low frequency electrostatic fluctuations in standard discharges have correlation lengths  $\sim 10$  cm [18], substantially larger than the width of the shear region. While there is no analytical theory that accounts for direct  $\mathbf{E} \times \mathbf{B}$  flow shear reduction of these fluctuations, such an interaction is conceivable and would significantly extend the applicability of the sheared-flow turbulence suppression paradigm [15]. These fluctuations may also be affected by favorable, but as yet unmeasured changes in edge gradients. Such changes could also account for the reduction of short wavelength fluctuations

beyond the shear region. The global, core-resonant  $m = 1$  magnetic fluctuations may also be directly affected by the  $\mathbf{E} \times \mathbf{B}$  flow shear. However, a more likely explanation is that this reduction results from the quasilinear edge current profile modification that occurs with each of the dominantly  $m = 0$  small dynamo events, in analogy with auxiliary poloidal current drive [4,19].

To summarize, RFP plasmas with increased energy and particle confinement exhibit a strongly inhomogeneous radial electric field and reduced electrostatic and magnetic fluctuations. The electrostatic fluctuation power decreases tenfold at all frequencies throughout the edge region ( $r/a > 0.84$ ) and twentyfold within the narrow  $\sim 2$  cm region of strong shear at  $r/a \approx 0.87$ . The magnetic fluctuations are reduced to a level approaching the minimum ever observed in the MST. Improved confinement from reduced magnetic fluctuations in the RFP is anticipated, owing to the measured dominance of magnetic-fluctuation-induced transport [1,2]. However, the dramatic reduction in electrostatic turbulence might also affect energy transport. Further measurements are required to understand the relative importance of electrostatic and magnetic fluctuations in these enhanced confinement discharges.

The authors are grateful to A. F. Almagri, J. T. Chapman, D. Craig, and the MST group for help with data acquisition and to G. Fiksel, D. J. Den Hartog, and P. W. Terry for useful discussions. This work was supported by the U.S. Department of Energy.

- [1] M. R. Stoneking *et al.*, Phys. Rev. Lett. **73**, 549 (1994).
- [2] G. Fiksel *et al.*, Phys. Rev. Lett. **72**, 1028 (1994).
- [3] J. S. Sarff *et al.*, Phys. Rev. Lett. **72**, 3670 (1994).
- [4] J. S. Sarff *et al.*, Phys. Rev. Lett. **78**, 62 (1997).
- [5] T. D. Rempel *et al.*, Phys. Rev. Lett. **67**, 1438 (1991).
- [6] R. J. Groebner, Phys. Fluids B **5**, 2343 (1993).
- [7] K. H. Burrell, Plasma Phys. Controlled Fusion **36**, A291 (1994).
- [8] B. E. Chapman *et al.*, Phys. Plasmas **3**, 709 (1996).
- [9] R. N. Dexter *et al.*, Fusion Technol. **19**, 131 (1991).
- [10] Y. Hirano *et al.*, Nucl. Fusion **36**, 721 (1996).
- [11] D. J. Den Hartog *et al.*, J. Nucl. Mater. **200**, 177 (1993); D. J. Den Hartog and R. D. Kendrick, *ibid.* **220-222**, 631 (1995).
- [12] S. Hokin *et al.*, Phys. Fluids B **3**, 2241 (1991).
- [13] R. R. Weynants *et al.*, in *Proceedings of the 13th International Conference on Plasma Physics and Controlled Nuclear Fusion Research, Washington, DC, 1990* (IAEA, Vienna, 1991), Vol. 1, p. 473.
- [14] F. L. Hinton and R. D. Hazeltine, Rev. Mod. Phys. **48**, 239 (1976).
- [15] H. Biglari, P. H. Diamond, and P. W. Terry, Phys. Fluids B **2**, 1 (1990).
- [16] T. S. Hahm and K. H. Burrell, Phys. Plasmas **2**, 1648 (1995).
- [17] K. H. Burrell *et al.*, Phys. Plasmas **4**, 1499 (1997).
- [18] D. Craig (private communication).
- [19] Y. L. Ho, Nucl. Fusion **31**, 341 (1991).